Vortical Fluid and Λ Spin Correlations in High-Energy Heavy-Ion Collisions

Long-gang Pang,[1] Hannah Petersen,[1,2,3] Qun Wang,[4] and Xin-Nian Wang[5,6]
[1]*Frankfurt Institute for Advanced Studies, Ruth-Moufang-Strasse 1, 60438 Frankfurt am Main, Germany*
[2]*Institute for Theoretical Physics, Goethe University, Max-von-Laue-Strasse 1, 60438 Frankfurt am Main, Germany*
[3]*GSI Helmholtzzentrum für Schwerionenforschung, Planckstrasse 1, 64291 Darmstadt, Germany*
[4]*Interdisciplinary Center for Theoretical Study and Department of Modern Physics, University of Science and Technology of China, Hefei, Anhui 230026, China*
[5]*Key Laboratory of Quark and Lepton Physics (MOE) and Institute of Particle Physics, Central China Normal University, Wuhan 430079, China*
[6]*Nuclear Science Division, MS 70R0319, Lawrence Berkeley National Laboratory, Berkeley, California 94720, USA*
(Received 16 May 2016; published 1 November 2016)

Fermions become polarized in a vortical fluid due to spin-vorticity coupling, and the polarization density is proportional to the local fluid vorticity. The radial expansion converts spatial vortical structures in the transverse plane to spin correlations in the azimuthal angle of final Λ hyperons' transverse momentum in high-energy heavy-ion collisions. Using a $(3+1)$D viscous hydrodynamic model with fluctuating initial conditions from a multiphase transport (AMPT) model, we reveal two vortical structures that are common in many fluid dynamic systems: a right-handed toroidal structure around each beam direction for transverse vorticity and pairing of longitudinal vortices with opposite signs in the transverse plane. The calculated azimuthal correlation of the transverse spin is shown to have a cosine form plus an offset due to the toroidal structure of the transverse vorticity around the beam direction and the global spin polarization. The longitudinal spin correlation in the azimuthal angle shows an oscillatory structure due to multiple vorticity pairs in the transverse plane. Mechanisms of these vortical structures, physical implications of hyperon spin correlations, dependence on colliding energy, rapidity, centrality, and sensitivity to the shear viscosity are also investigated.

DOI: 10.1103/PhysRevLett.117.192301

Introduction.—The large orbital angular momentum in noncentral high-energy heavy-ion collisions can lead to fluid shear and nonvanishing local fluid vorticity [1–13]. In such a vortical fluid, the spin-vorticity coupling polarizes the spin of fermions (quarks and baryons) [1–11] along the direction of the vorticity.

The mechanism of fermion polarization in a vortical fluid is very similar to the chiral vortical effect [14–19]. The axial current induced by vorticity leads to the local polarization effect [19] as a result of the spin-vorticity coupling for chiral or massless fermions [20]. The spin polarization density for massive fermions can be shown to be directly proportional to the local vorticity [21,22]. Consequently, final-state baryons such as hyperons should also be polarized along the direction of the local fluid vorticity at the freeze-out hypersurface. Measurements of the final-state hyperon polarization, which are feasible through the parity-violating decay [23], will shed light on the vortical structure and transport properties of the strongly coupled quark-gluon plasma (sQGP) in high-energy heavy-ion collisions.

In this Letter, we investigate the vortical structure of the sQGP in high-energy heavy-ion collisions in a $(3+1)$D viscous hydrodynamic model with fluctuating initial conditions from the a multiphase transport (AMPT) model [24]. We show that the transverse vorticity of the sQGP has a toroidal structure around beam directions due to radial expansion of the fluid with large longitudinal flow velocity in addition to the net vorticity along the direction of the global orbital angular momentum of noncentral collisions. The longitudinal vorticity, however, has multiple vortex pairs with opposite signs in the transverse plane due to the convective radial flow of hot spots. We propose using the spin correlation of two hyperons in the azimuthal angle in momentum space to study these vortical structures since radial expansion of the system and spin-vorticity coupling convert spatial vortical structures into spin correlations in the azimuthal angle of final hyperons. We will calculate hyperon spin correlations in the azimuthal angle and study their dependence on collision energy, rapidity, centrality, and shear viscosity. We neglect the spin polarization due to magnetic fields in this study.

Fermion polarization in a vortical fluid.—Interactions in a medium with local vorticity polarize a fermion's spin due to spin-orbital coupling [1]. In thermal equilibrium, such a coupling between spin and local vorticity effectively shifts the energy level of fermions with different spin states. This leads to different phase space distributions for fermions with different spin states and, therefore, spin polarization along the direction of the local vorticity [21]. One can calculate the spin polarization in thermal equilibrium within a quantum kinetic approach [22].

In the quantum kinetic theory, the fermion distribution in the absence of electromagnetic interaction is described by the Wigner function $W(x,p)$ in space-time x and the 4-momentum p,

$$W_{\alpha\beta}(x,p)=\int\frac{d^4y}{(2\pi)^4}e^{-ipy}\left\langle\bar{\psi}_\beta\left(x+\frac{1}{2}y\right)\psi_\alpha\left(x-\frac{1}{2}y\right)\right\rangle, \tag{1}$$

where $\psi(x)$ and $\bar{\psi}(x)$ are fermionic fields and $\langle\cdots\rangle$ denotes the ensemble average. Using the Dirac equation for a fermion with mass m, one can derive the quantum kinetic equation for the fermion's Wigner function [25,26],

$$\left[\gamma_\mu\left(p^\mu+\frac{i}{2}\hbar\partial_x^\mu\right)-m\right]W(x,p)=0. \tag{2}$$

The Wigner function is a 4×4 matrix in Dirac space and can be decomposed into 16 independent generators of the Clifford algebra. The coefficients correspond to the scalar, pseudoscalar, vector, axial vector, and tensor components, respectively. The kinetic equation for the Wigner function in Eq. (2) will lead to a system of equations for these components which can be solved through a gradient expansion. The spin polarization is given by the axial component of the Wigner function. At next-to-leading order in gradient expansion, one obtains [22] the polarization density for the on-shell fermions,

$$\Pi^\mu(x)=\hbar\frac{\omega^\mu}{2}\beta\int\frac{d^3p}{(2\pi)^3}f_{\rm FD}(x,p)[1-f_{\rm FD}(x,p)], \tag{3}$$

where the vorticity is defined as $\omega^\mu=\tilde{\Omega}^{\mu\nu}u_\nu/\beta$, $\tilde{\Omega}^{\mu\nu}=\frac{1}{2}\epsilon^{\mu\nu\rho\sigma}\partial_\rho(\beta u_\sigma)$, and $f_{\rm FD}(x,p)$ is the Fermi-Dirac distribution,

$$f_{\rm FD}(x,p)=\frac{1}{e^{\beta[u\cdot p\mp\mu]}+1}, \tag{4}$$

for fermions $(-)$ and antifermions $(+)$ on their mass shell with the chemical potential μ, the temperature $T=1/\beta$, and the fluid four-velocity u_μ. The energy splitting between two spin states due to spin-vorticity coupling is proportional to local vorticity. Therefore, the spin polarization density is proportional to the vorticity vector and the fermion number susceptibility at the next-to-leading order in gradient expansion.

In a hydrodynamic model of high-energy heavy-ion collisions, one can calculate the average polarization vector for final spin-1/2 hadrons with the momentum p [21,22],

$$P^\mu(p)\equiv\frac{d\Pi^\mu(p)/d^3p}{dN/d^3p}=\frac{\hbar}{4m}\frac{\int d\Sigma_\sigma p^\sigma\tilde{\Omega}^{\mu\nu}p_\nu f_{\rm FD}(x,p)[1-f_{\rm FD}(x,p)]}{\int d\Sigma_\sigma p^\sigma f_{\rm FD}(x,p)}, \tag{5}$$

where $d\Sigma_\sigma$ is the differential volume vector on the Cooper-Frye hypersurface at the hadronic freeze-out temperature T_f. We will work in the Bjorken-Milne coordinate wtih $X^\mu=(\tau,x,y,\eta)$, where $\tau=\sqrt{t^2-z^2}$ and the spatial rapidity is defined as $\tanh\eta=z/t$.

$(3+1)$D *viscous hydrodynamic model.*— We use the newly developed Central China Normal University (CCNU)–Lawrence Berkeley National Laboratory viscous (CLVisc) hydrodynamic model with fluctuating initial conditions from the AMPT model. The CLVisc hydrodynamic model [27] is a viscous extension of an ideal $(3+1)$D hydrodynamic model [28] that parallelizes the Kurganov-Tadmor algorithm [29] for hydrodynamic evolution and Cooper-Frye particlization on graphics processing units (GPUs) using OpenCL (Open Computing Language for parallel programming of heterogeneous systems). In this study, we use time steps $\Delta\tau=0.005$ fm, the transverse spacing $\Delta x=\Delta y=0.1$ fm, and the longitudinal spacing $\Delta\eta=0.1$. The number of grid points are 301, 301, and 181 for the x, y, and η directions, respectively.

The initial conditions for the CLVisc model are constructed from the AMPT model [24] at an initial proper time τ_0, with Gaussian smearing in both transverse coordinates and spatial rapidity. The overall normalization of the initial conditions on the energy-momentum tensor is adjusted to fit the final charged hadron multiplicity at midrapidity in the most central collisions and kept fixed for all other centralities [28]. The initial thermalization time is set at $\tau_0=0.4$ fm at the RHIC energies and $\tau_0=0.2$ fm at the LHC. The partial chemical equilibrium EOS $s95p$-PCE165-$v0$ parametrizing lattice QCD calculations [30] is used in the CLVisc model. We also assume a zero baryon chemical potential and a hadronic freeze-out temperature $T_f=137$ MeV. In the CLVisc simulations presented in this Letter, we have neglected the vorticity term in the viscous stress tensor. We have also neglected viscous corrections to the final hadron spectra in the calculation of hyperon spin polarization. Both of these higher order effects can be included in future studies.

The AMPT model uses the heavy-ion jet interaction generator (HIJING) [31] for the initial parton production from both incoherent semihard scatterings and coherent string formation. A string-melting mechanism is used to convert strings into partons which undergo parton transport processes before hadronization through parton coalescence. Therefore, the AMPT initial conditions for CLVisc simulations at the initial proper time τ_0 contain fluctuations in both the transverse and longitudinal directions. The longitudinal variation of the initial energy density leads to

decorrelation of anisotropic flow of final hadrons with large pseudorapidity gaps [32,33].

Convective flow and vorticity distribution.—The initial conditions constructed from the AMPT-HIJING model contain fluctuations in the local fluid velocity [32] due to string breaking and minijets. These fluctuations in fluid velocity and the energy density lead to nonvanishing local vorticity as well as global net vorticity along the orbital angular momentum of noncentral collisions [13].

According to the definition of the vorticity ω^{μ}, it has contributions from convection (the spatial gradient of the fluid velocity), acceleration (the temporal gradient of the fluid velocity), and conduction (the spatial and temporal gradient of the temperature). Within the CLVisc calculations, we find that the vorticity is dominated by convection. The system develops large longitudinal fluid velocity quickly along the beam directions in the early time, while the transverse gradient in the initial energy density also leads to a buildup of a radial component of the fluid velocity. This convective fluid velocity field gives rise to a transverse vorticity distribution that has a right-handed toroidal structure (ringlike) around each beam direction. Shown in Fig. 1 as arrows are distributions of $\vec{\omega}_{\perp}(x,y)$ in the transverse plane at a spatial rapidity $\eta = 4$ and a proper time $\tau = 3$ fm/c in a semiperipheral (20%–30%) Au + Au collision at $\sqrt{s_{NN}} = 200$ GeV from the CLVisc simulations. One can clearly see the right-handed toroidal structure (module fluctuations) around the beam direction (out of the transverse plane). The total net vorticity $\langle \sum \omega_y \rangle$ projected to the reaction plane is nonzero for noncentral collisions.

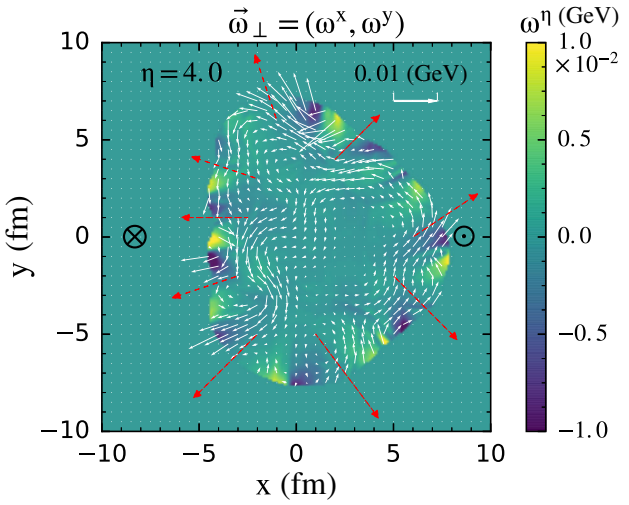

FIG. 1. Transverse (arrows) and longitudinal vorticity (contour) distributions in the transverse plane at $\eta = 4$ in semiperipheral (20%–30%) Au + Au collisions at $\sqrt{s_{NN}} = 200$ GeV with shear viscosity to entropy density ratio $\eta_v/s = 0.08$. Dashed arrows indicate the radial flow of hot spots. A cutoff in energy density $\epsilon > 0.03$ GeV/fm^3 is imposed. The direction of the beam (target) is out of plane (⊙) [into the plane (⊗)]. The orbital angular momentum of the collision is along $-\hat{y}$.

The magnitude of the local transverse vorticity $\vec{\omega}_{\perp}$ and the net total vorticity $\langle \sum \omega_y \rangle$ should both increase with centrality, spatial rapidity, and decreasing energy [13].

Similarly, the collective flow of the hot spots (denoted by dashed arrows in Fig. 1) can also lead to convective flow in the radial direction. Because of approximate local boost invariance of the fluid, this leads to pairings of the positive and negative longitudinal vorticity ω_{η}'s, or vortex pairings, in the transverse plane at a given spatial rapidity, shown as colored contours in Fig. 1. Such vortex pairing is essentially a 2D manifestation of a 3D toroid of vorticity elongated in the longitudinal direction. Since the longitudinal vorticity is caused mainly by transverse fluctuations, its magnitude and structure should depend on centrality but not on colliding energy and rapidity. The average value over the entire transverse plane $\langle \sum \omega_{\eta} \rangle$, however, should vanish.

Hyperon spin correlation.—Since the spin polarization is directly proportional to the local vorticity, the spatial structure in Fig. 1 is expected to show up in the azimuthal correlation of Λ spin polarization due to radial expansion, which correlates the spatial azimuthal angle of the fluid cells to the azimuthal angle of final hadron's transverse momentum. Therefore, we propose using the spin correlations of two Λ's to study the vortical structure of the expanding fluid in high-energy heavy-ion collisions. Shown in Fig. 2 are the transverse and longitudinal spin correlations of two Λ's, $\langle \vec{P}_{\perp}(\phi_1) \cdot \vec{P}_{\perp}(\phi_2) \rangle$ and $\langle P_{\eta}(\phi_1) P_{\eta}(\phi_2) \rangle$, respectively, as functions of the azimuthal angle difference $|\phi_1 - \phi_2|$ of their momenta. In our CLVisc hydrosimulations of semicentral (20%–30%) Pb + Pb collisions at $\sqrt{s_{NN}} = 2.76$ TeV, we have set the shear viscosity to entropy density ratio to $\eta_v/s = 0.08$ (the solid lines) and 0.0 (the dashed lines). As expected, the transverse spin correlation in azimuthal angle has an approximate cosine form due to the toroidal structure of the transverse vorticity around the beam direction plus an offset due to the global spin polarization. Both the amplitude of the oscillation (the local polarization) and the offset (the global polarization) increase with rapidity as well as with η_v/s. The longitudinal spin correlation, on the other hand, displays a different behavior. The oscillation in $|\phi_1 - \phi_2|$ is the result of vortex pairing in the transverse plane, as illustrated in Fig. 1. The sign change at $|\phi_1 - \phi_2| \approx 1$ indicates the typical opening angle of the vortex pairs from the convective radial flow due to transverse geometry and fluctuations. The rise of the correlation at large angles is the result of spin correlations from different vortex pairs in the transverse plane. The amplitude of the longitudinal spin correlation increases slightly with rapidity but decreases slightly with η_v/s.

In Fig. 3, we show (a) the Λ transverse spin correlations in the rapidity range $Y \in [2,3]$ and (b) the longitudinal spin correlation in $Y \in [0,1]$ in semiperipheral (20%–30%) and central (0%–5%) Au + Au collisions at $\sqrt{s_{NN}} = 62.4$,

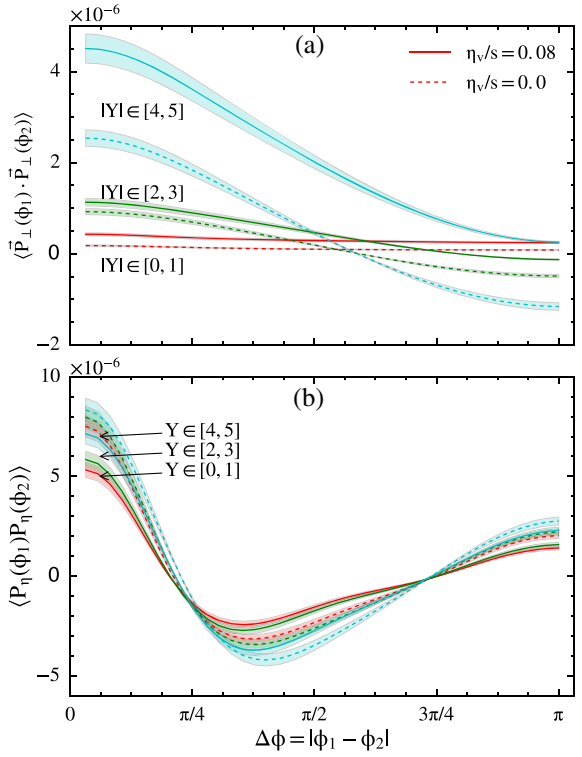

FIG. 2. (a) Transverse and (b) longitudinal spin correlation of two Λ's as a function of the azimuthal angle difference (of their momenta) in different rapidity regions of semiperipheral (20%–30%) Pb + Pb collisions at $\sqrt{s_{NN}} = 2.76$ TeV with the shear viscosity to entropy density ratios $\eta_v/s = 0.08$ (solid curves) and 0.0 (dashed curves). Shaded areas indicate statistical errors with 200 hydroevents.

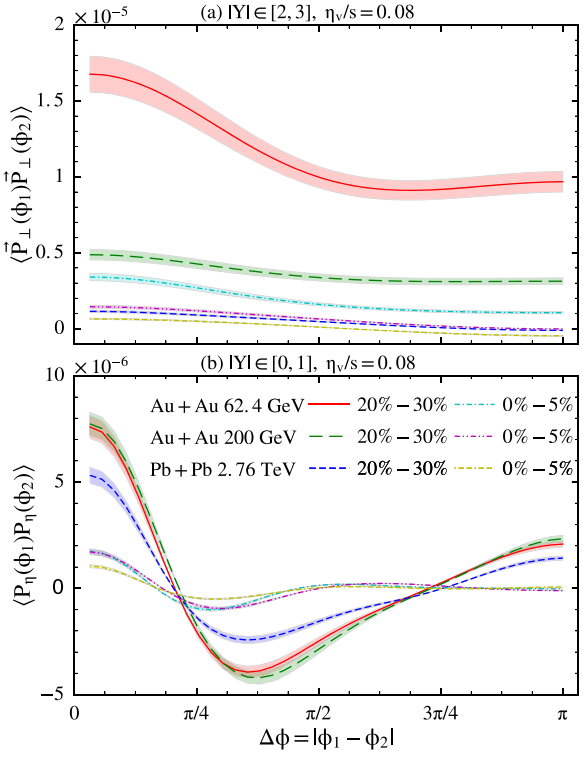

FIG. 3. (a) Transverse ($|Y| \in [2, 3]$) and (b) longitudinal ($|Y| \in [0, 1]$) spin correlation of two Λ's as a function of the azimuthal angle difference (of their momenta) in semiperipheral (20%–30%) and central (0%–5%) Au + Au collisions at $\sqrt{s_{NN}} = 62.4$, 200 GeV, and Pb + Pb collisions at $\sqrt{s_{NN}} = 2.76$ TeV with $\eta_v/s = 0.08$. Shaded areas indicate statistical errors with 200 hydroevents.

200 GeV, and Pb + Pb collisions at $\sqrt{s_{NN}} = 2.76$ TeV for $\eta_v/s = 0.08$. Both the amplitude and the offset of the transverse spin correlation increase with a decreasing colliding energy because the transverse vorticity is bigger due to larger longitudinal fluctuations at lower beam energies or larger rapidities. They also have a strong centrality dependence and become very small in central collisions. The longitudinal spin correlation in the central rapidity region, however, does not have a strong energy dependence because of the geometric and fluctuating nature of its origin. It has a strong dependence on the centrality. In noncentral collisions, the vortex pairing is dominated by the dipole structure of the elliptic flow, and the opening angle $\Delta\phi \sim 3\pi/8$ indicates the scale of the vortex pair. In central collisions, the vortex pairing is dominated by hot spots, and the angular structure of the longitudinal spin correlations indicates the size and the distance between these hot spots.

Summary and discussions.—In this Letter, we study the vortical structure of the sQGP fluid in high-energy heavy-ion collisions using the CLVisc hydrodynamic model, with fluctuating initial conditions from the AMPT-HIJING model. The transverse vorticity has a right-handed toroidal structure around each beam direction, in addition to the average net vorticity along the reaction plane due to global orbital angular momentum in noncentral collisions. The longitudinal vorticity has a vortex-pairing structure in the transverse plane. We propose using the Λ spin correlations to measure these vortical structures. We predict both the transverse and longitudinal spin correlations as functions of the azimuthal angle difference of two Λs' momenta. Measurements of these spin correlation functions can give us a detailed picture of the flow and vortical structure and provide important constraints on the initial condition and the transport properties of the dense matter in high-energy heavy-ion collisions. We limit our predictions to high-energy heavy-ion collisions, where one can neglect the finite baryon chemical potential. For collisions at the beam scan energies at the RHIC, one has to include baryon number conservation and an EOS with a finite baryon chemical potential in hydrodynamic simulations. Our simulations indicate, however, that the magnitude of the local spin polarization will increase at lower beam energies. We also do not include the vorticity term in the shear stress tensor or viscous corrections to the phase-space distribution of the final hadrons. We neglect the effect of the magnetic field on the spin polarization, which should be small during

the hadronic freeze-out following equilibrium hydrodynamic evolution. These effects can be addressed in more accurate studies in the future.

This work is supported in part by NSFC under Grants No. 11221504 and No. 11535012, by MOST of China under Grant No. 2014DFG02050, by MSBRD in China under Grants No. 2015CB856902, No. 2014CB845404, and No. 2014CB845402, by the U.S. DOE under Contract No. DE-AC02-05CH11231, by Helmholtz Young Investigator Group VH-NG-822 from the Helmholtz Association and GSI, and by HIC for FAIR within the framework of the Landes-Offensive zur Entwicklung Wissenschaftlich-Oekonomischer Exzellenz (LOEWE) program launched by the State of Hesse. Computations are performed at the Green Cube at the GSI and GPU workstations at CCNU.

[1] Z.-T. Liang and X.-N. Wang, Phys. Rev. Lett. **94**, 102301 (2005); **96**, 039901(E) (2006).
[2] Z.-T. Liang and X.-N. Wang, Phys. Lett. B **629**, 20 (2005).
[3] J.-H. Gao, S.-W. Chen, W.-T. Deng, Z.-T. Liang, Q. Wang, and X.-N. Wang, Phys. Rev. C **77**, 044902 (2008).
[4] F. Becattini and L. Ferroni, Eur. Phys. J. C **52**, 597 (2007).
[5] B. Betz, M. Gyulassy, and G. Torrieri, Phys. Rev. C **76**, 044901 (2007).
[6] F. Becattini, F. Piccinini, and J. Rizzo, Phys. Rev. C **77**, 024906 (2008).
[7] X.-G. Huang, P. Huovinen, and X.-N. Wang, Phys. Rev. C **84**, 054910 (2011).
[8] L. P. Csernai, V. K. Magas, and D. J. Wang, Phys. Rev. C **87**, 034906 (2013).
[9] F. Becattini, L. P. Csernai, and D. J. Wang, Phys. Rev. C **88**, 034905 (2013).
[10] F. Becattini, G. Inghirami, V. Rolando, A. Beraudo, L. Del Zanna, A. De Pace, M. Nardi, G. Pagliara, and V. Chandra, Eur. Phys. J. C **75**, 406 (2015).
[11] Y. Xie, R. C. Glastad, and L. P. Csernai, Phys. Rev. C **92**, 064901 (2015).
[12] Y. Jiang, Z.-W. Lin, and J. Liao, arXiv:1602.06580 [Phys. Rev. C (to be published)].
[13] W.-T. Deng and X.-G. Huang, Phys. Rev. C **93**, 064907 (2016).
[14] D. E. Kharzeev, L. D. McLerran, and H. J. Warringa, Nucl. Phys. **A803**, 227 (2008).
[15] K. Fukushima, D. E. Kharzeev, and H. J. Warringa, Phys. Rev. D **78**, 074033 (2008).
[16] D. T. Son and P. Surowka, Phys. Rev. Lett. **103**, 191601 (2009).
[17] D. E. Kharzeev and D. T. Son, Phys. Rev. Lett. **106**, 062301 (2011).
[18] S. Pu, J.-H. Gao, and Q. Wang, Phys. Rev. D **83**, 094017 (2011).
[19] J.-H. Gao, Z.-T. Liang, S. Pu, Q. Wang, and X.-N. Wang, Phys. Rev. Lett. **109**, 232301 (2012).
[20] J.-H. Gao and Q. Wang, Phys. Lett. B **749**, 542 (2015).
[21] F. Becattini, V. Chandra, L. Del Zanna, and E. Grossi, Ann. Phys. (Amsterdam) **338**, 32 (2013).
[22] R.-H. Fang, L.-G. Pang, Q. Wang, and X.-N. Wang, Phys. Rev. C **94**, 024904 (2016).
[23] B. I. Abelev *et al.* (STAR Collaboration), Phys. Rev. C **76**, 024915 (2007).
[24] Z.-W. Lin, C. M. Ko, B.-A. Li, B. Zhang, and S. Pal, Phys. Rev. C **72**, 064901 (2005).
[25] H.-T. Elze, M. Gyulassy, and D. Vasak, Nucl. Phys. **B276**, 706 (1986).
[26] D. Vasak, M. Gyulassy, and H.-T. Elze, Ann. Phys. (N.Y.) **173**, 462 (1987).
[27] L.-G. Pang, Y. Hatta, X.-N. Wang, and B.-W. Xiao, Phys. Rev. D **91**, 074027 (2015).
[28] L. Pang, Q. Wang, and X.-N. Wang, Phys. Rev. C **86**, 024911 (2012).
[29] A. Kurganov and E. Tadmor, J. Comput. Phys. **160**, 241 (2000).
[30] P. Huovinen and P. Petreczky, Nucl. Phys. **A837**, 26 (2010).
[31] X.-N. Wang and M. Gyulassy, Phys. Rev. D **44**, 3501 (1991).
[32] L.-G. Pang, G.-Y. Qin, V. Roy, X.-N. Wang, and G.-L. Ma, Phys. Rev. C **91**, 044904 (2015).
[33] L.-G. Pang, H. Petersen, G.-Y. Qin, V. Roy, and X.-N. Wang, Eur. Phys. J. A **52**, 97 (2016).